DOA Estimation of Low Altitude Target Based on Bounded Component Analysis Algorithm

Eren Babatas[1,2]***, Alper T. Erdogan***[1]

[1]*Koc University, Istanbul, Turkey*
[2]*Aselsan Inc., Ankara, Turkey*

Keywords: Blind Source Separation, Bounded Component Analysis, Direction Of Arrival Estimation

Abstract

A recently introduced Blind Source Separation method, called Bounded Component Analysis, is used as preliminary technique to isolate direct path radar wave from ground reflected waves in order to overcome the multipath effect. This method enables the radar to estimate the target angle without any a priori knowledge of the operation environment. The numerical experiments illustrate the potential benefit of the proposed approach relative to classical maximum likelihood method (CMLM) based on free space propagation model.

1 Introduction

Direction Of Arrival (DOA) estimation of a low altitude target is still a current issue that engages researchers' attention. While estimating the DOA of low altitude target, radar receive two or more coherent echoes via multipath. This results the received signals to be faded and strengthened cyclically while target propagation. Many researchers have investigated the multipath effects on radar and suggested various approaches to reduce the estimation errors in DOA estimation brought by these effects. The methods based on these approaches can be classified in three main categories: Monopulse methods, parametric methods and subspace methods. The classical maximum likelihood method (CMLM) [1] is classified as a parametric method and can distinguish coherent signals. The CMLM solves the maximum likelihood function in order to maximize the correlation between array manifold matrix and received data. However, the CMLM does not show a good performance if the direct-path and reflected-path echoes, which are coherent signals, fade each other.

In this paper, a Blind Source Separation (BSS) technique named Bounded Component Analysis (BCA) is taken into consideration to separate the direct-path and reflected-path echoes which can improve the performance of the CMLM in the fading case. BCA is a recently introduced BSS scheme that utilizes the boundedness property of sources to replace the usual independence assumption with a weaker assumption, allowing separation of both dependent and independent sources [2]. In [3], a geometric BCA framework is introduced which can separate both independent and dependent sources from their mixtures where the mixing system is instantaneous. This approach is based on the assumption that bounded source vectors lie in a rectangular l_∞ norm ball. Since radar echoes are bounded by Effective Radiation Power (ERP), this BCA framework is applicable to the multipath problem. We combine this approach with the CMLM [1] to solve the low angle problem. The proposed algorithm weakens the influence of the multipath attenuation and improves the performance of low-angle estimation.

2 Multipath Signal Model

Griesser and Balanis' model [4] is taken as the multipath signal model. Assumed geometry by the model is given in fig. 1 below. As shown in fig. 1, a uniform linear array (ULA) and a

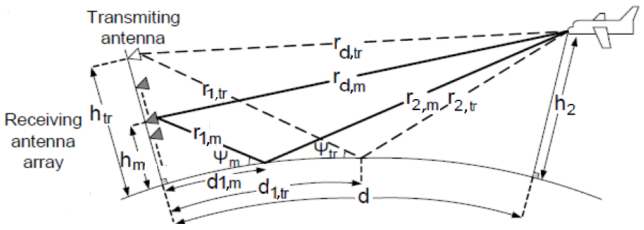

Fig. 1: Multipath signal model for radar wave propagation.

point target are utilized. In transmitting and receiving, there are two ways between the antenna and the target, i.e., direct-way $(r_{d,tr}, r_{d,m})$ and reflection-way $(r_{1,tr} + r_{2,tr}, r_{1,m} + r_{2,m})$. Reflection angles are represented with ψ_{tr}, ψ_m. The earth is modelled as a sphere with radius R_e. The reflection coefficient of the spherical earth, $\rho(n, \psi)$, is a complex variable.

For the geometrical calculation of the reflection angles ψ_{tr}, ψ_m, we use the approximate formulas given in [4]. The reflection coefficient $\rho(n, \psi)$ is the sum of two components called specular reflection coefficient (ρ_s) and diffuse reflection coefficient (ρ_d).

$$\rho(n, \psi) = \rho_s(\psi) + \rho_d(n) \tag{1}$$

The specular reflection coefficient is calculated with the subsequent equations:

$$\rho_s(\psi) = \rho_0 R_s(\psi) = \Gamma D R_s(\psi) \tag{2}$$

$$R_s(\psi) = \exp(-8\pi^2\delta(\psi)^2) I_0(-8\pi^2\delta(\psi)^2) \tag{3}$$

$$\delta(\psi) = (\sigma_h \sin\psi)/\lambda \tag{4}$$

where Γ is the Fresnel reflection coefficient, D is the divergence factor, $I_0(z)$ is the modified Bessel function, σ_h is the effective surface height, and λ is the wavelength for the operational frequency. The diffuse reflection coefficient is a more complicated parameter defined with the equation

$$\begin{aligned} \rho_d(n) &= \rho_0 R_d(n) \\ &= \Gamma_{v,h} D R_d(n) \\ &= \Gamma_{v,h} D(R_{dx}(n) + jR_{dy}(n)) \end{aligned} \tag{5}$$

where R_{dx} and R_{dy} are zero mean Gaussian random processes. By using these definitions and **narrowband assumption**, the signal arrived at the elements of an M-element ULA from a point target is expressed with

$$\mathbf{x}(\mathbf{n}) = \left[\ x_1(n), x_2(n), \cdots, x_M(n)\ \right]^T \tag{6}$$

$$x_k(n) = o(n)\{\exp(-jKr_{d,k}) + \rho(n,\psi)\exp(-jK(r_{1,k}+r_{2,k}))\}$$

where $o(n)$ is the radar wave which can be in any waveform and $K = \frac{2\pi}{\lambda}$ is the wave number for the operational frequency.

The multipath signal model for ULA in (6) can be attributed as a BSS mixture model. The overall reflection coefficient in (1) is said to be dependent on time and the grazing angle. Let us define $\mathbf{r}_d = [r_{d,1}, r_{d,2}, \ldots, r_{d,M}]^T$ and $\psi = [\psi_1, \psi_2, \ldots, \psi_M]^T$. Note that $r_{1,k}$ and $r_{2,k}$ parameters are dependent on ψ_k as can be seen in figure 1. The sum of direct-path and reflected-path echoes would be expressed dependent on the sampling time n, $\mathbf{r}_d$ and ψ.

$$\mathbf{x}(n, \mathbf{r}_d, \psi) = \tag{7}$$

$$o(n)\begin{bmatrix} \exp(-jKr_{d,1}) + \rho(n,\psi)\exp(-jK(r_{1,1}+r_{2,1})) \\ \vdots \\ \exp(-jKr_{d,M}) + \rho(n,\psi)\exp(-jK(r_{1,M}+r_{2,M})) \end{bmatrix}$$

$$\mathbf{H}(\mathbf{r}_d, \psi) = \tag{8}$$

$$\begin{bmatrix} \exp(-jKr_{d,1}) & \exp(-jK(r_{1,1}+r_{2,1})) \\ \vdots & \\ \exp(-jKr_{d,M}) & \exp(-jK(r_{1,M}+r_{1,M})) \end{bmatrix}$$

$$\mathbf{s}(n,\psi) = \begin{bmatrix} o(n) \\ \rho(n,\psi)o(n) \end{bmatrix} \tag{9}$$

$$\mathbf{x}(n, \mathbf{r}_d, \psi) = \mathbf{H}(\mathbf{r}_d, \psi)\mathbf{s}(n,\psi) \qquad n = 1, \ldots, L. \tag{10}$$

where $\mathbf{H}(\mathbf{r}_d, \psi)$ is named the mixing channel response and $\mathbf{s}(n,\psi)$ is named the source signal vector in BSS problem. In the next section we make it clear that (10) is a special case of BSS problem based on linear mixture model, under the assumption ($\mathbf{A1}$).

Assumption 1: Variation in $\mathbf{H}(\mathbf{r}_d, \psi)$ with respect to the parameters $\mathbf{r}_d$ and ψ throughout receiving L samples from the target is ignorable ($\mathbf{A1}$).

3 Framework and Iterative Algorithm for BCA

In the instantaneous BSS setup given in the article [3]

- We assume that there are p sources, where there are L samples of these sources represented by the set $\mathcal{S} = \{\mathbf{s}(n) \in \Re^p, n = 1, \ldots L\}$. Furthermore, it is assumed that source vectors are bounded in magnitude and lie in a bounding hyper-rectangle, i.e.,

$$\mathbf{s}(n) \in \mathcal{B}_s, \qquad n = 1, \ldots, L, \tag{11}$$

$$\mathcal{B}_s = \{\mathbf{q} \in \Re^p : \hat{\mathbf{I}}_s \leq \mathbf{q} \leq \hat{\mathbf{u}}_s\}. \tag{12}$$

  where $\hat{\mathbf{I}}_s$ and $\hat{\mathbf{u}}_s$ are the vectors containing minimum and maximum values for the components of the source vectors in $\mathcal{S}$ respectively. Note that, we do not make any stochastic assumption about the source vector such as independence of its components. This makes our main assumption valid for the multipath problem case in which the direct and reflected echoes are coherent.
- The mixing system is linear and memoryless which is represented by the matrix $\mathbf{H} \in \Re^{qxp}$. We assume that $q \geq p$ and $\mathbf{H}$ is full rank, i.e., the number of channels is more than the number of sources.
- The mixtures are represented with

$$\mathbf{y}(n) = \mathbf{H}\mathbf{s}(n), \qquad n = 1, \ldots, L. \tag{13}$$

- $\mathbf{W} \in \Re^{pxq}$ is the separator matrix, and its outputs are represented with

$$\mathbf{z}(n) = \mathbf{W}\mathbf{y}(n), \quad n = 1, \ldots L. \tag{14}$$

- By defining the cascade of the mixing and separator systems as $\mathbf{G} = \mathbf{WH}$, we can write the separator outputs in terms of sources as

$$\mathbf{z}(n) = \mathbf{G}\mathbf{s}(n), \quad n = 1, \ldots, L. \tag{15}$$

We refer to perfect separator as a $\mathbf{W}$ matrix for which the corresponding $\mathbf{G} = \mathbf{WH}$ is in the form

$$\mathbf{G} = \mathbf{PD}, \tag{16}$$

where $\mathbf{P}$ is a permutation matrix and $\mathbf{D}$ is a full rank diagonal matrix. In [3], for the purpose of obtaining the perfect separator, the volume ratio of two geometric objects defined over the separator output samples referred as principal hyper-ellipsoid $\mathcal{E}_z$ and bounding hyper-rectangle $\mathcal{B}_z$ is utilized. These geometric objects and the framework can be seen in figure 2. Based on these definitions, we define the BCA objective as the volume ratio

$$\bar{J}(\mathbf{W}) = \text{Volume}(\mathcal{E}_z)/\text{Volume}(\mathcal{B}_z) \tag{17}$$

$$= C_p \frac{\sqrt{\det(\hat{\mathbf{R}}(Z_\mathbf{G}))}}{\prod(\hat{R}(Z_\mathbf{G}))} \tag{18}$$

where $C_p = \pi^{p/2}/\Gamma(p/2+1)$, $\hat{\mathbf{R}}(Z_\mathbf{G})$ is the covariance matrix of the separator outputs, and the range vector $\hat{R}(Z_\mathbf{G})$ contains

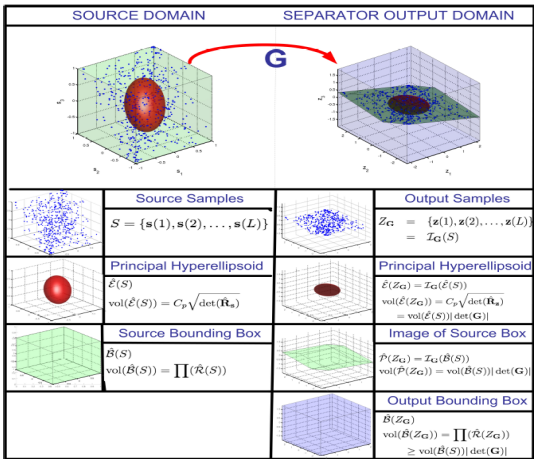

Fig. 2: Geometric objects for the proposed BCA framework.

the side lengths of the bounding hyper-rectangle. Dropping the dimension dependent constant C_p, the new objective is obtained as

$$J(\mathbf{W}) = \frac{\sqrt{\det(\hat{\mathbf{R}}(Z_{\mathbf{G}}))}}{\prod(\hat{R}(Z_{\mathbf{G}}))}. \quad (19)$$

In order to ensure the global optimality of the perfect separators with respect to the objective in (19), we define the following **local dominance** assumption:

Assumption 2: Source sample set $\mathcal{S}$ contains the vertices of the bounding hyper-rectangle $\mathcal{B}_s$ (**A2**).

Now, the following theorem shows that all global optima of (19) are perfect separators.

Theorem: Given $\mathbf{H}$ is full-rank and (**A2**) is correct, then all global maxima of (19) are perfect separators.

The mathematical proof of the theorem that the separator matrices maximizing the objective in (19) is available in [3].

Although $\mathcal{J}(\mathbf{W})$ is non-convex and not differentiable everywhere, we can still utilize Clarke sub-differential [6] for deriving iterative algorithms.

$$\mathbf{W}^{(t+1)} = \mathbf{W}^{(t)} + \mu^{(t)}((\hat{\mathbf{R}}_z^{(t)})^{-1}\mathbf{W}^{(t)}\hat{\mathbf{R}}_y - \sum_{m=1}^{p} \frac{1}{\hat{R}_m(Z_{\mathbf{G}^{(t)}})}\mathbf{e}_m(\mathbf{y}(k_{m,+}^{(t)}) - \mathbf{y}(k_{m,-}^{(t)}))) \quad (20)$$

where $\hat{\mathbf{R}}_y = \frac{p}{L}\sum_{n=1}^{L}\mathbf{y}(n)\mathbf{y}(n)^T - \mu_y\mu_y^T$ with $\mu_y = \frac{1}{L}\sum_{n=1}^{L}\mathbf{y}(n)$, $\mathbf{y}(k_{m,+}^{(t)})$ and $\mathbf{y}(k_{m,-}^{(t)})$ represent the mixture signals for which the separator output reaches its maximum and minimum values at the (t) iteration respectively. This equation is formulated for real sources, however the received echoes by the uniform linear array are complex. In the complex case, we consider p complex sources whose real and complex components have finite support. For this case, we define the operators $\Upsilon : C^p \rightarrow \Re^{2p}$, $\Upsilon(\mathbf{x}) = [\mathrm{Re}(\mathbf{x}^T)\ \mathrm{Im}(\mathbf{x}^T)\ ]^T$ and $\Gamma : C^{pxq} \rightarrow \Re^{2px2q}$, $\Gamma(\mathbf{A}) = \begin{bmatrix}\mathrm{Re}(\mathbf{A}) & -\mathrm{Im}(\mathbf{A})\\ \mathrm{Im}(\mathbf{A}) & \mathrm{Re}(\mathbf{A})\end{bmatrix}$. By applying these operators, we transform our problem to real domain.

In multipath problem, the specular component is fully coherent with the direct-path echo. This fact reveals an analogy between the radar multipath problem and the mixing problem of two dependent sources.

4 Proposed Method for Low Altitude DOA Estimation

By utilizing the analogy between the multipath model (10) and the BSS model (13) under the assumption (**A1**), we propose an approach in four steps for estimating the DOA of a low-altitude target.

I- Estimate the separator matrix $\mathbf{W}$ by (20) to separate direct-path and reflected-path echoes with the MxL size signal matrix received by an $Mx1$ antenna array.

II- Extract the direct-path and reflected-path echoes given in (9). Let's name the extracted echoes as $z_1(n)$ and $z_2(n)$.

III- Estimate the signal vectors $\mathbf{x}_1(n)$ and $\mathbf{x}_2(n)$ that contain phase differences between the array elements for the direct-path and reflected-path echoes:

$$\mathbf{x}_1(n) = (\mathbf{W}(1,:)^H\mathbf{W}(1,:))^{-1}\mathbf{W}(1,:)^H z_1(n) \qquad n = 1, \ldots, L. \quad (21)$$

$$\mathbf{x}_2(n) = (\mathbf{W}(2,:)^H\mathbf{W}(2,:))^{-1}\mathbf{W}(2,:)^H z_2(n) \qquad n = 1, \ldots, L. \quad (22)$$

IV- As we dont know which signal vector corresponds to the direct-path echo, we estimate DOAs for both signal vectors $\mathbf{x}_1(n)$ and $\mathbf{x}_2(n)$ by using any free-space model based DOA estimation method. We use the CMLM in [1] for DOA estimation. The angle with larger value will be assigned as the target DOA.

5 Simulation Results

In the analyses, we illustrate DOA estimation performance of the proposed method in comparison to the free-space model based CMLM and Beamspace Domain Maximum Likelihood (BDML) in [5]. The setup used in the simulations is defined as follows: i)-75-element Uniform Linear Array, inter-element distance = 0.5λ, ii)-Radar Height (38th element)=16 m, iii)-Frequency = 10 GHz, iv)-Swerling-0 case:Constant target RCS, SNR changes only range dependently, v)-Sea state = 0 (no diffuse reflection).

In the first numerical example, we hold the target range constant at 5500 meters, free-space input Signal-to-Noise Ratio (SNR) at 20 dB and change the target altitude. Overall input SNR (direct-path + reflected-path) versus the target DOA is given fig. 3. While taking L samples from the target for the BCA algorithm, the target moves in the direction of the array. The supplemental parameters used are

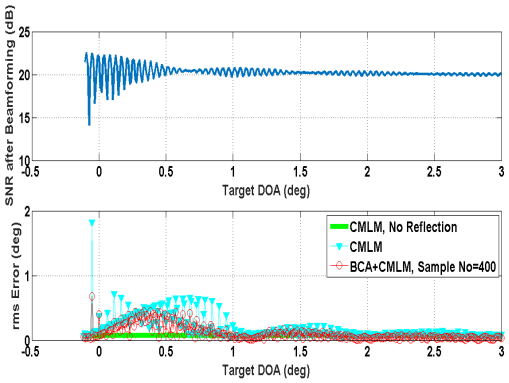

Fig. 3: Performance improvement with BCA. 1)-Signal-to-Noise Ratio vs target DOA at target-range=5500m, 2)-RMS error vs target DOA at target-range=5500m.

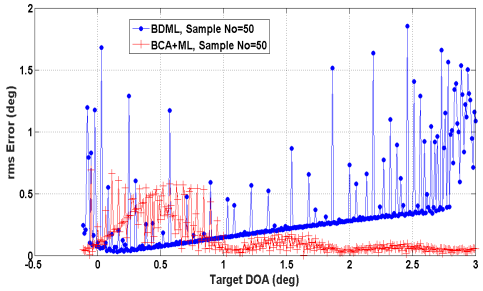

Fig. 4: Performance comparison of (BCA+CMLM) & BDML. RMS error vs target DOA at target-range=5500m.

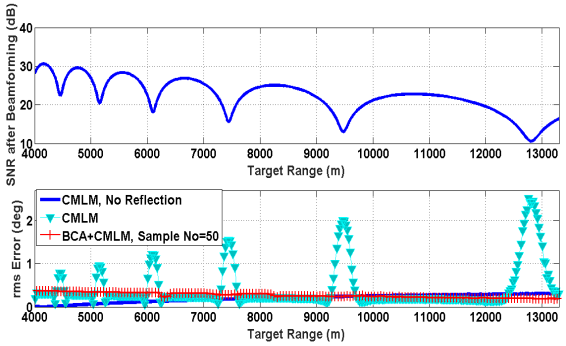

Fig. 5: Performance improvement with BCA. 1)-Signal-to-Noise Ratio vs target range at target-altitude=30m, 2)-RMS error vs target range at target-altitude=30m.

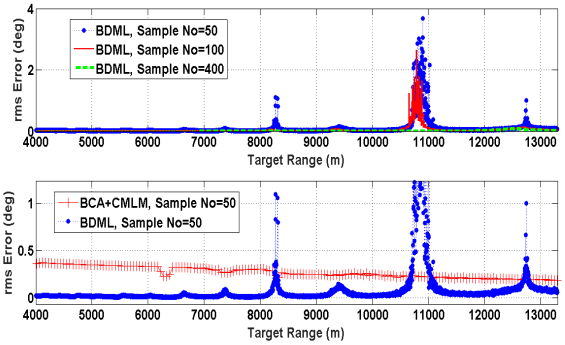

Fig. 6: Performance comparison of (BCA+CMLM) & BDML. RMS error vs target range at target-altitude=30m.

i)-Target range=5500 m, ii)-Target altitude=5 m-300 m, iii)-Target Velocity=300 m/s, iv)-Sampling Time=0.5e-3 s, v)-ML search interval=$-\tan^{-1}(\frac{Radar-altitude}{Target-range}) : 0.1^\circ : 5^\circ$. The second plot of fig. 3 depicts the root-mean-square (rms) error graphs of CMLM with and without multipath effect, and (BCA+CMLM) for different number of samples. We can comment that the proposed method provides considerable improvement with respect to CMLM under multipath effect, especially at low angles. Since the reflected-path echo weakens at high altitudes, the free-space model becomes to be more acceptable and (BCA+CMLM) show close performance with CMLM. In fig. 4, (BCA+CMLM) is compared to BDML method. It is evident that BDML is inferior to (BCA+CMLM) for small amount of samples which creates low integrated SNR. In the multipath problem, likelihood function gets an ambigious pattern in the low SNR case, and it causes gross estimation errors that can be seen in fig. 4.

In the second numerical example, we hold the target altitude constant at 30 meters, take free-space input Signal-to-Noise Ratio (SNR) 20 dB at 13.3 km. The target moves in the direction of the array and overall SNR changes with the target range. Overall input SNR (direct-path + reflected-path) versus the target range is given fig. 5. DOA estimation process begins after taking first L samples from the target. Beginning with the (L+1)th sample, a sliding window is applied to collect L samples for the BCA algorithm. The supplemental parameters used in this example are i)-Target range=[13300 m:-(Target Velocity * Sampling Time) m:4000 m], ii)-Target altitude=30 m, iii)-Target Velocity=300 m/s, iv)-Sampling Time=10e-3 s, v)- ML search interval=$-\tan^{-1}(\frac{Radar-altitude}{Target-range}) : 0.1^\circ : 5^\circ$. Fig. 5 depicts that (BCA+CMLM) improves the performance of CMLM at the ranges where direct-path and reflected-path echoes fade each other. Lastly, in fig. 6, it is shown that (BCA+CMLM) outperforms BDML at some range intervals where BDML performance shows large excursions because of the same reason as that in the first example.

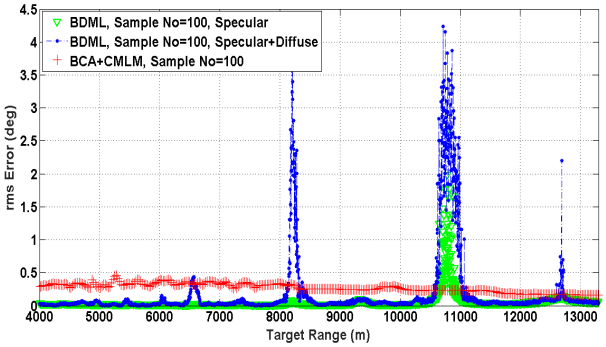

Fig. 7: Performance comparison of (BCA+CMLM) & BDML under specular+diffuse reflection. RMS error vs target range for target-altitude=30m and σ_h =50cm.

In the third numerical example, the simulation parameters except reflection coefficient are the same with those in the second example. We add the diffuse effect to the reflection by taking the rms height σ_h in (4) as 50 cm. Then the total reflection coefficient is the sum of specular and diffuse compo-

nents. BDML assumes the reflection is fully specular while BCA works without such an assumption. That's why we can expect for BDML the more diffuse effect, the worse performance. This case is shown clearly in fig. 7.

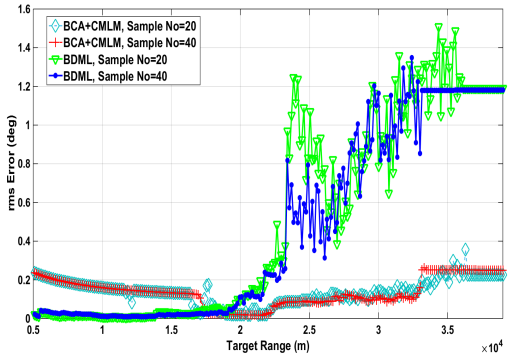

Fig. 8: Performance comparison of (BCA+CMLM) & BDML in Swerling-1 case. RMS error vs target range for target-altitude=30m.

In the fourth numerical example, the target RCS model is changed to be Swerling-1. We again hold the target altitude constant at 30 meters again, but for this time, the target velocity is 1500 m/s. Since the target is very fast, we extend the initial range interval to 39 km and use less samples for source separation. We take free-space input Signal-to-Noise Ratio (SNR) 20 dB at 39 km. As in the first and second examples, the reflection includes only specular effect. The supplemental parameters used in this example are i)-Target range=[39000 m:-(Target Velocity * Sampling Time) m:4000 m], ii)-Target altitude=30 m, iii)-Target Velocity=1500 m/s, iv)-Sampling Time=100e-3 s, v)- ML search interval=$-\tan^{-1}(\frac{Radar-altitude}{Target-range}) : 0.1^\circ : 5^\circ$, vi)- Frequency=10 GHz. Looking at the fig. 8, it is concluded that (BCA+CMLM) is not effected from the RCS fluctuation in the Swerling-1 case. On the other hand, BDML's performance deteriorates at long ranges where input SNR is low so that BDML can not solve the ambiguity caused by the reflection and the RCS fluctuation.

6 Conclusions

In this article, we proposed a deterministic Bounded Component Analysis approach to solve the low angle estimation problem. The proposed approach aims to isolate direct-path target echo from the reflected-path target echo in order to overcome the multipath effect. Since the framework is defined only with respect to separator output samples, it does not need any knowledge about the operation environment, target and multipath model. The numerical examples demonstrate the improvement over the Classical Maximum Likelihood Method especially at long ranges where echoes fade each other and overall SNR is low. Beside it, the practical relative merit of the proposed framework over Beamspace Domain Maximum Likelihood method, particularly for small amount of samples, is exhibited.

References

[1] P. Stoica, K.C. Sharman. "Maximum likelihood methods for direction-of-arrival estimation", *IEEE Transactions Acoustics Speech Signal Process.*, **vol. 38**, pp. 1132-1143 (1990).

[2] S. Cruces. "Bounded Component Analysis of Linear Mixtures: A Criterion for Minimum Convex Perimeter", *IEEE Transactions on Signal Processing*, **vol. 58**, pp. 2141-2154, (2010).

[3] Alper T. Erdogan. "A Class of Bounded Component Analysis Algorithms for Separation of Both Independent and Dependent Sources", *IEEE Transactions on Signal Processing*, **vol. 61**, pp. 5730-5743, (November 2013).

[4] T. Griesser, C.C. Balanis. "Oceanic Low-Angle Monopulse Radar Tracking Errors", *IEEE Journal of Oceanic Engineering*, **vol. 12**, pp. 289-295 (1987).

[5] Michael D. Zoltowski, Ta-Sung Lee. "Maximum Likelihood Based Sensor Array Signal Processing in the Beamspace Domain for Low Angle Radar Tracking", *IEEE Transactions on Signal Processing*, **vol. 39**, pp. 656-671 (March 1991).

[6] Adil Bagirov, Napsu Karmitsa, Marko M. Mäkelä. "Introduction to Nonsmooth Optimization: theory, practice and software", *Springer*, (2014).